ELSEVIER

Journal of Hazardous Materials A138 (2006) 423–432

Journal of Hazardous Materials

www.elsevier.com/locate/jhazmat

Acoustic emission detection of microcrack formation and development in cementitious wasteforms with immobilised Al

L.M. Spasova *, M.I. Ojovan

Immobilisation Science Laboratory, Department of Engineering Materials, University of Sheffield, Mappin Street, Sheffield S1 3JD, UK

Received 25 March 2006; received in revised form 23 May 2006; accepted 23 May 2006
Available online 2 June 2006

Abstract

An acoustic emission (AE) technique was applied for early detection, characterisation and time progress description of cracking phenomenon caused by the corrosion of Al encapsulated in cement matrix. The study was conducted on an ordinary Portland cement (OPC) system encapsulating high purity Al bar. Acoustic signals were generated and released during immersing of the sample in deionised water. A computer controlled PCI-2 based AE system processed the signals detected by piezoelectric transducers. A subsequent comparative study of the AE data collected with those obtained from a reference OPC sample has been applied. Recorded AE activity confirmed that the process of initiation and development of Al corrosion causes significant mechanical stresses within the cement matrix. Our analysis demonstrated possibility to differentiate AE signals based on their characteristics, and potentially correlate detected AE with the fracture processes in the cement system encapsulating Al.

Keywords: AE technique; Cementitious wastefroms; Al corrosion; Microcrack formation and development

1. Introduction

Cementation, bituminisation and vitrification are commercially available technologies for immobilisation of radioactive wastes [1]. Hydraulic cements have been used over many years for encapsulation of low and intermediate level radioactive waste (LILW) due to their favorable chemical and physical properties [1–10]. In the UK LILWs are typically encapsulated in cement matrix to produce solid wasteforms [3,8,9]. However corrosion of encapsulated radioactive metals such as Al, Mg and their alloys, arising from spent nuclear fuel reprocessing, in the high pH environment of cement matrix potentially causes loss of mechanical strength of cementitious wasteforms [9]. Since durability is one of the most important requirements for safe storage and wasteform long-term disposal [1] different composite cements have been extensively studied [3,8,9]. Nevertheless reliable methods for early detection of damage initiation and development applied to cementitious wasteforms encapsulating metallic wastes would be of significant benefit.

AE technique based on detection of transient acoustic waves generated and released during microcracking and other irreversible structural changes is widely used as a nondestructive method for materials research [11,12]. Moreover AE technique has been proved as a valuable tool to study the fracture processes in materials and particularly in cement-based structures [13–22]. The mechanical behavior of generic cement materials during deformation and rupture is related to their heterogeneity and can be explained in term of microcrack and macrocrack nucleation and development [13]. Microcracks are typically formed at relatively low stress level. As the stress intensity increases the microcracks are localized to initiate development of visible cracks, which further grow and eventually lead to structural failure. An AE activity presented by cumulative AE events number and energy has been used to determine the onset and extend of the damage induced under loading in cement-based structures [14,15]. On the other hand acoustic characteristics such as duration, amplitude and counts number have been applied to identify different failure mechanisms at various stress levels and to relate generated and released AE with different processes presented in cement-based materials under stress [16].

The high sensitivity of AE technique to microcrack nucleation and propagation is a main advantage applied for continuous monitoring of concrete structural integrity. Based on AE data

* Corresponding author. Tel.: +44 114 222 5990; fax: +44 114 222 5943.
E-mail address: mtp05lms@sheffield.ac.uk (L.M. Spasova).

0304-3894/$ – see front matter © 2006 Elsevier B.V. All rights reserved.
doi:10.1016/j.jhazmat.2006.05.067

collected several modeling approaches for prediction of concrete fracture behavior have been developed [18,19]. Moreover Landis and Baillon [15] reported for a relationship between the AE and the fracture energy in order to apply AE as a tool for quantitative damage measurements in concrete materials. They observed a significant jump in the detected AE energy when a peak loading has been achieved. An important alteration of the AE energy rate during postpeak loading has been also distinguished. Landis and Baillon associated the later phenomena with microcrack forming processes resulted in the onset of critical crack growth followed by a change of the dominant source of AE energy from fracture to "noncrack forming energy dissipation processes". Tam and Weng [14] and Wu et al. [22] found a good correlation between the time progress of AE activity and the mechanical performance of concrete specimens with different aggregates under compression. They associated the significant increase observed in the total number of detected AE events with "unstable cracking" of the structure when its ultimate strength has been achieved. In order to summarize the main sources of AE activity in generic cement structures under loading were attributed to different failure mechanisms caused by processes such as [13–22]:

(a) microcrack initiation and development including microflaws aggregation, microcrack formation, steady growth and coalescence and formation of visible cracks. As it is reported in [16,22] the later processes generated large number of AE signals with relatively short duration and low amplitude in comparison with the signals associated with
(b) crack(s) extension, reinforcement breaking or pullout, distinguished by detection of high energetic signals in less population [16].

Corrosion of steel reinforcement is one of the main issues of serviceability of concrete structures. AE technique has been applied for detection and identification of concrete cracking due to corrosion of reinforcing steel [23–26]. Detected AE was associated with several events such as:

(a) infiltration of the aggressive solution through the cement porosity followed by modification of the medium at metal/concrete interface and initiation of the corrosion process;
(b) accumulation of corrosion products which results in an increase of the compressive forces at reinforcement/concrete interface leading to microcrack initiation;
(c) friction of the corrosion products along the walls of these cracks and cement pores;
(d) microscopic crack propagation.

In addition the initiation and development of different type corrosion processes such as pitting, exfoliation and galvanic corrosion of aluminum alloys have been also an object of extensive AE monitoring and analysis [27–29]. The processes generated AE were related with:

(a) friction and release of hydrogen bubbles formed during corrosion characterised with low amplitude and rise time signals in high population in comparison with the signals due to
(b) crack propagation and evolution of hydrogen bubbles.

Finally AE technique was used to characterise and predict the accumulation of strength during solidification of concrete [31,32] and early hydration of cement paste [33–35]. Nevertheless the applications of AE in the nuclear waste management field are still limited. An example is the study performed by Belov and Aloy [36] concerned with the feasible application of this nondestructive method for quality control of glass and ceramics for waste immobilisation. However no comparative study of AE signals characteristics and possible relationship between AE activity and stresses induced in the cement matrix due to corrosion of encapsulated Al have ever been made.

The objectives of the present work are to assess the mechanical performance of cement matrix encapsulating Al in terms of AE; to identify the processes which initiate microcrack formation and development based on the number of AE events, energy detected and analysis on the acoustic characteristics such as duration, peak of amplitude and counts number; to compare the results obtained from the cement sample encapsulating Al with those collected from the reference cement sample.

2. Experimental procedure

Pure ordinary Portland cement (OPC) has been used for preparation of two samples on a laboratory scale, one with encapsulated Al and a reference sample. Water to powder mass ratio applied was 0.33 providing required mechanical strength of the rigid products used for immobilisation of metallic wastes [1,2,9]. High purity Al (99.999%) was chosen to minimize any possible effects of cement on the Al corrosion process in presence of alloying elements. The cement was mixed and then poured into 100 ml capacity plastic containers with airtight lids and Al rod placed inside. Cylindrical samples with 65 mm height and 60 mm diameter were formed. Then the samples were cured at 20 and 40 °C in environmental chambers for more than 6 months for the cement sample with encapsulated Al and at about 2 months for the reference sample.

AE was monitored by two transducers plugged into preamplifiers further connected with the active channels of a computer controlled PCI-2 based AE system, supplied and calibrated by PAC (Physical Acoustics Corp.). The transducers applied were a broadband (WD) and R15D from PAC, attached to the samples under AE monitoring as shown in Fig. 1. Acoustic waves and their parameters such as amplitude, duration, rise time, counts number and absolute energy were recorded on a hard drive. For each detected AE signal following acoustic parameters were used for postprocessing:

- AE event duration: time interval between the first and the last threshold level crossing;

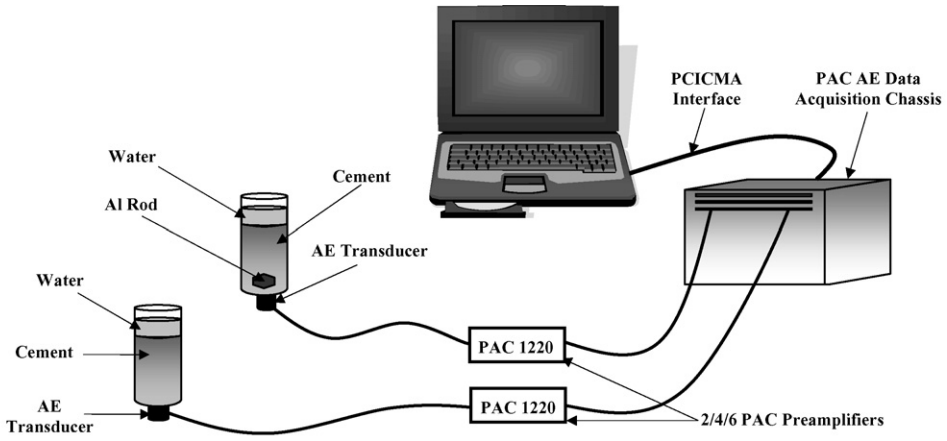

Fig. 1. Experimental setup.

- Counts number (N_{counts}): ring down count over the AE event duration;
- Peak of AE wave amplitude: magnitude of the most energetic component of the wave given in dB;
- Absolute energy (E_{ABS}): quantifiable measurement of the energy contained in an AE hit derived as an integral of the squared voltage signal divided by the reference resistance (10 kΩ) over the duration of the AE waveform packet and performed in atto joules (10^{-18} J);
- AE hits number (N_{hits}): number of registered AE signals;
- Average absolute energy per hit ($E_{\text{ABS,av}}$) calculated by

$$E_{\text{ABS,av}} = \frac{\text{Total } E_{\text{ABS}}}{\text{Total } N_{\text{hits}}}$$

where Total E_{ABS} is the sum of the absolute energies of all AE hit divided by their total number (Total N_{hits}) for a particular interval of the test duration.

The threshold level for AE data acquisition was set up at 40 dB. The same value of amplification was also established for the preamplifiers. A good acoustic coupling of the transducers with the external bottom surface of the plastic containers was provided by a thin layer of grease.

Under our experimental conditions, carried out at room temperature, the same amount (50 ml) of deionised water was poured in the plastic containers followed by the commencement of AE data acquisition.

3. Results and analysis

During the test duration established for 51.5 h 5340 AE hits were detected from the cement sample with encapsulated Al and 5423 from the reference sample. The curves representative of the cumulated number of AE hits (N_{hits}) and absolute energy (E_{ABS}) versus time for the cement sample with encapsulated Al and the reference sample are plotted respectively in Figs. 2 and 3.

The number of AE hits and associated absolute energy detected from the cement sample with encapsulated Al (Fig. 2) was not constant in time with clearly defined periods of an increase followed by intervals of very low AE activity. A similar pattern has been reported by Ing et al. [24] and related with a consequence of periods of crack extension within concrete structures followed by accumulation of corrosion products on

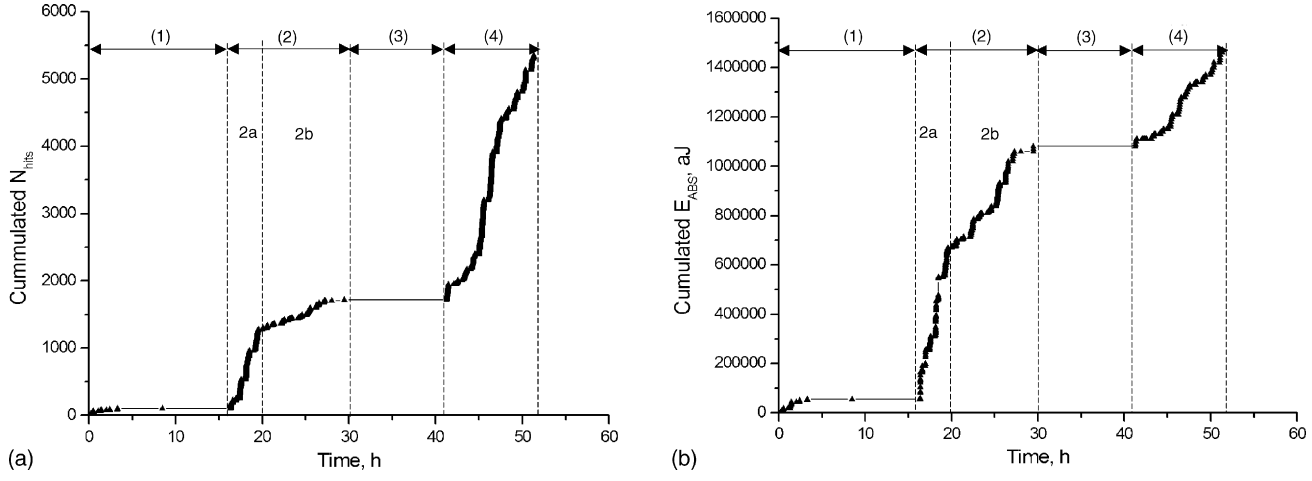

Fig. 2. Cumulated AE hits number (a) and absolute energy (b) vs. time for the cement sample with encapsulated Al.

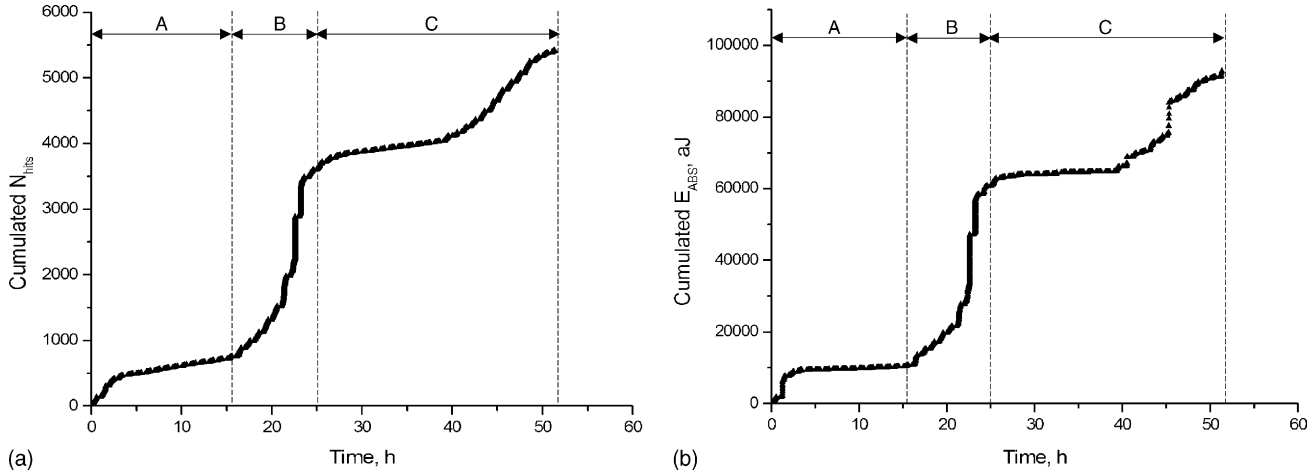

Fig. 3. Cumulated AE hits number (a) and absolute energy (b) vs. time for the reference cement sample.

reinforcing steel surface. However the AE activity from the reference sample was characterised with continuous increasing rate but also performed with a sequence of periods with discriminative number of the detected AE hits (Fig. 3).

The common trends of alteration (high or low) in the AE activity and amount of detected absolute energy from the cement sample with encapsulated Al was used to distinguish four stages in the history of conducted AE monitoring (Fig. 2). For the first time we applied a procedure based on acoustic characteristics to analyse our data from each of the determined stages. This procedure for differentiation of failure mechanisms within cement-based materials under mechanical loading was developed by Wu et al. [16]. The method, which is used to relate specific mechanisms of fracture in concrete structures and AE characteristics of detected signals [16], suggests that:

(i) for the same AE activity, the higher the energy the higher the amplitude of detected signals and the longer their duration;
(ii) AE activity associated with the same failure mechanism has the same acoustic characteristics.

The diagram of the identification procedure developed in [16] is given in Fig. 4.

To differentiate mechanisms generating AE a number of filters are set for the duration of signals in the range of several μs. When a certain duration range is selected, three graphs are drawn: (i) the number of AE hits versus amplitude (in dB), (ii) the counts number versus amplitude (in dB) and (iii) the hits versus counts. Then the shapes of the curves obtained on these three graphs are compared. If the peak of hits versus amplitude graph (A) has the same value as that from the counts versus amplitude graph (B) the average number of counts per hit (C) has to be determined by dividing the total number of AE hits to total number of counts. Furthermore if calculated value (C) matches with the peak of counts versus hits graph (D) one fracture mechanism which corresponds to an AE activity within the selected duration range can be determined. For all other cases identification of the mechanism initiating AE cannot be done.

The results obtained for the AE activities from the cement wasteform samples analysed by use of identification procedure from [16] are discussed below.

3.1. AE data analysis for the cement sample with encapsulated Al

The first determined stage (stage 1 from Fig. 2) with relatively long duration of 16.5 h corresponded to a low AE activity containing about 2% of the total number of detected AE hits. Table 1 summarises the results from the procedure (Fig. 4) applied for the AE signals detected during this stage. It was found that the signals with short duration between 0 and 20 μs and respectively low amplitude of 41 dB are in most high population. As previously reported [25,26] this type of signals can be associated with water infiltration through the porosity of the cement structure and modification of the medium at metal/cement interface followed by activation of Al corrosion. Additionally the accumulation of corrosion products resulting in an increase of the compressive forces on the metal/cement interface causes microcrack nucleation and growth of the pre-existing microcracks, voids or other defects within the cement matrix [25]. Moreover the friction of the corrosion products and formed hydrogen bubbles along the inner side of these cracks and cement pores also can be responsible for generation and release of AE waves [24,25]. The later processes can be correlated with identified signals with longer duration between 21 and 200 μs and amplitude peak of 44 and 45 dB. The last three groups of more energetic signals, however, given in Table 1 are likely to be generated by microscopic crack propagation and hydrogen bubbles evolution [27–30].

Stage 2 with duration of 13.5 h is characterised with significant increase in the AE activity presented by 30% of the total AE hits number and 68.6% of the total absolute energy. Moreover the graphs in Fig. 2a and b show a meaningful difference of the AE hits and absolute energy rate after about 20 h from the commencement of our AE data acquisition. The last finding was used to divide the second stage in two periods with duration respectively 3.5 and 10 h.

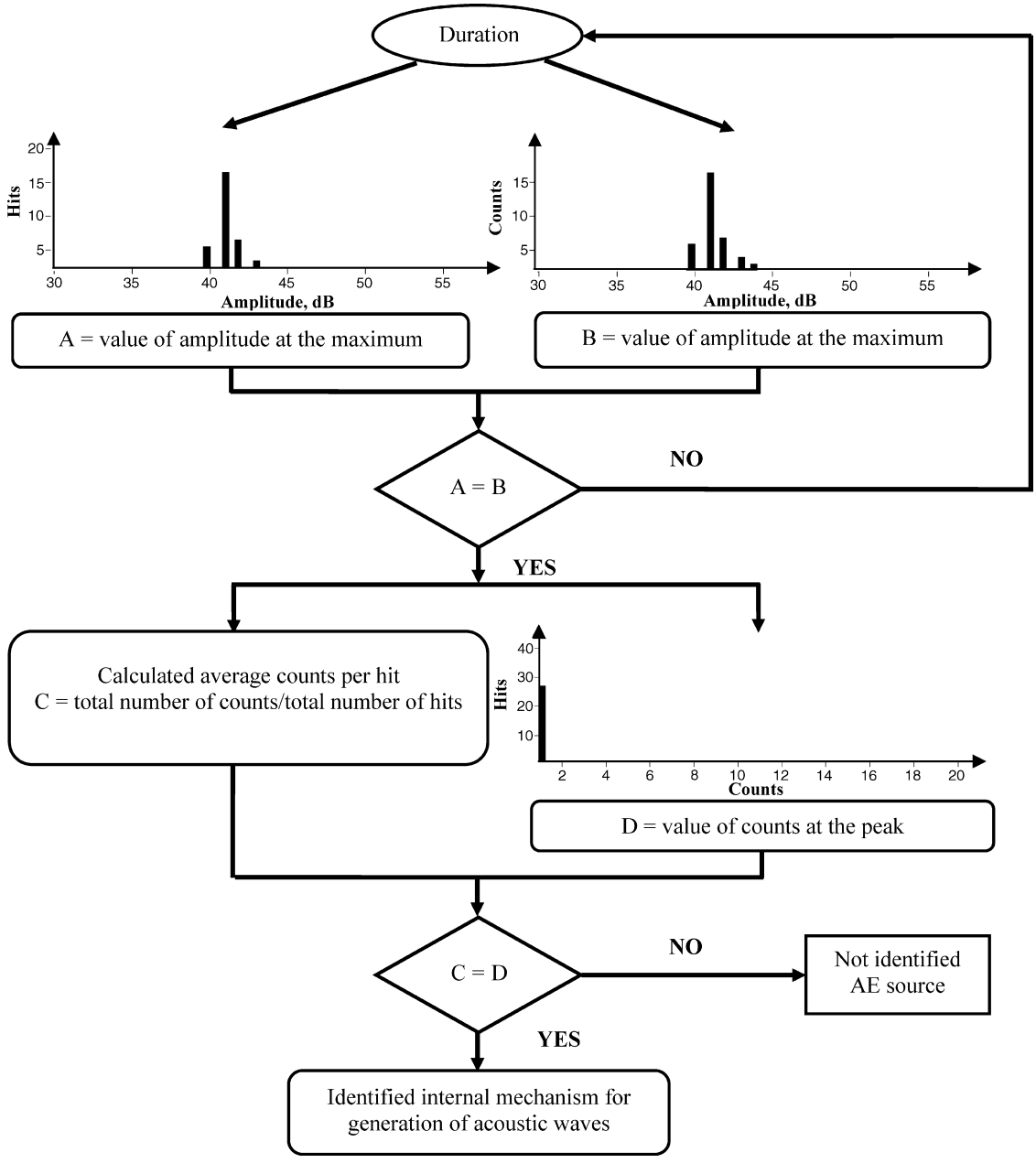

Fig. 4. The procedure for identification of an internal mechanism initiating AE applied for cement-based materials [16].

Table 1
AE characteristics for the signals detected during the stage 1

Time period	Hits duration (μs)	Amplitude peak (dB)	Amplitude range (dB)	Maximum no. of counts/hits	Calculated average counts/hits	N_{hits}	N_{counts}	% of total N_{hits}	Total E_{ABS} (aJ)	$E_{ABS,av}$ (aJ)
	0–20	41	40–44	1	1	27	27	0.5	857	31.74
	21–50	43	40–44	2	2	15	30	0.28	771	51.4
	51–80	44	40–45	3	3	8	24	0.15	611	76.37
0–16.5 h	81–200	45	43–47	4	4.21	14	59	0.26	1130	80.71
	201–300	46	43–49	6	6.61	13	86	0.24	2570	197.7
	301–700	48	45–57	11	11	9	99	0.17	7870	874.44
	701–1549	60	44–61	Not determined[a]	17.5	16	280	0.3	40700	2543.7
Total						102	605	1.9	54509	–

[a] The criteria for identification of an internal mechanism initiated AE are not satisfied.

Table 2
AE characteristics for the signals detected during the stage 2, period 2a

Time period	Hits duration (μs)	Amplitude peak (dB)	Amplitude range (dB)	Maximum no. of counts/hits	Calculated average counts/hits	N_{hits}	N_{counts}	% of total N_{hits}	Total E_{ABS} (aJ)	$E_{ABS,av}$ (aJ)
16.5–20 h	0–20	41	40–42	1	1.05	94	99	1.76	2790	29.68
	21–50	42	40–44	2	1.95	228	445	4.27	10000	43.86
	51–80	43	40–46	3	2.93	391	1147	7.33	27000	69.05
	81–200	44	40–48	4	4.27	230	982	4.31	20800	90.43
	201–300	47	42–51	6	6.69	62	415	1.16	13600	219.35
	301–500	50	41–55	10	9.68	47	455	0.88	25700	546.81
	501–700	59	40–61	15	15.46	62	959	1.16	123720	1995.5
	701–4650	Not determined[a]	40–66	Not determined[a]	29.06	59	1715	1.11	392710	6656.1
Total						1173	6217	21.98	616320	–

[a] The criteria for identification of an internal mechanism initiated AE are not satisfied.

During the first period (2a) the hits rate was about 335 hits/h. A large number of detected AE signals have duration in the range 21–200 μs and peak of amplitude from 42 to 44 dB (Table 2). Moreover a significant jump in the AE hits number compared with the previous stage has been observed. A very similar alteration in the AE activity is reported from conducted AE monitoring during loading of concrete structures [14,20,22]. The later phenomenon is associated with microcrack development and localization resulting in the onset of a critical crack(s) within the structures. We can suppose that under our experimental conditions the stress intensity in result of accumulation of corrosion products on the Al surface approached a level when a zone of fracture within cement matrix has been formed, making easier microcrack continuous growth and propagation. Additional evidences for this assumption are the cracks observed on the sample surface at the end of the test shown in Fig. 5.

During the second period (2b) of stage 2 the hits rate was significantly lower in comparison with that from the first period (about 43 hits/h). The AE signals in largest population during this time interval are characterised by amplitude peak of 56 dB and a duration between 301 and 600 μs (Table 3). These energetic signals can be associated with emissive hydrogen bubbles evolution and crack(s) extension within the cement structure. Moreover Landis and Baillon [15] reported very similar change in the amount of detected AE energy at about 40% of the post-peak loading as this observed during stage 2b (Fig. 2b) and related it with the dominant role of energy dissipation mechanisms such as friction, aggregate interlock and cracks bridging over the fracture processes within concrete under compression. However in our cement system the hydrogen bubbles evolution and friction along the walls of the crack(s) formed are the most

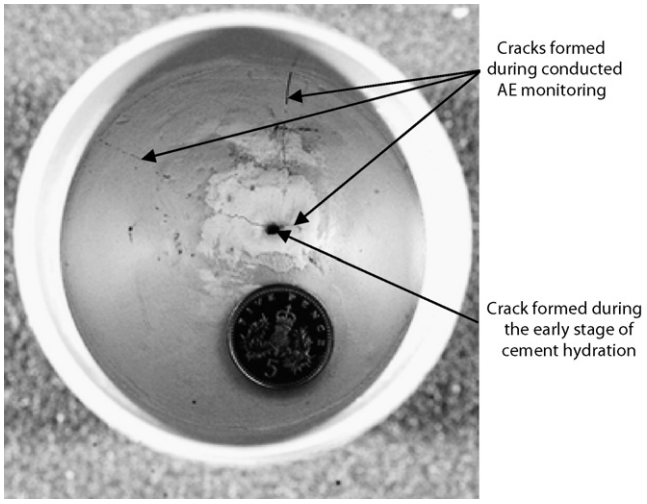

Fig. 5. Cracking of the cement sample with encapsulated Al after 51.5 h of AE monitoring (5p coin included for scale).

Table 3
AE characteristics for the signals detected during the stage 2, period 2b

Time period	Hits duration (μs)	Amplitude peak (dB)	Amplitude range (dB)	Maximum no. of counts/hits	Calculated average counts/hits	N_{hits}	N_{counts}	% of total N_{hits}	Total E_{ABS} (aJ)	$E_{ABS,av}$ (aJ)
20–30 h	0–20	41	40–41	1	1.02	46	47	0.86	1290	28.04
	21–50	42	40–43	2	1.85	46	85	0.86	2480	53.91
	51–200	43	40–45	3	3.44	52	179	0.97	5190	99.81
	201–300	47	40–49	6	6.31	35	221	0.655	9260	264.57
	301–600	56	40–59	13	13.74	222	3050	4.16	285730	1287.1
	601–700	58	56–60	20	19[a]	18	342	0.33	51800	2877.8
	701–1293	Not determined[a]	54–61	Not determined[a]	20.54	11	226	0.21	36500	3318.2
Total						430	4150	8.05	392250	–

[a] The criteria for identification of an internal mechanism initiated AE are not satisfied.

Table 4
AE characteristics for the signals detected during the stage 3

Time period	Hits duration (μs)	Amplitude peak (dB)	Amplitude range (dB)	Maximum no. of counts/hits	Calculated average counts/hits	N_{hits}	N_{counts}	% of total N_{hits}	Total E_{ABS} (aJ)	$E_{ABS,av}$ (aJ)
30–41 h	17–729	Not determined[a]	43–60	Not determined[a]	12.17	12	146	0.23	19800	1650

[a] The criteria for identification of an internal mechanism initiated AE are not satisfied.

Table 5
AE characteristics for the signals detected during the stage 4

Time period	Hits duration (μs)	Amplitude peak (dB)	Amplitude range (dB)	Maximum no. of counts/hits	Calculated average counts/hits	N_{hits}	N_{counts}	% of total N_{hits}	Total E_{ABS} (aJ)	$E_{ABS,av}$ (aJ)
41–51.5 h	0–20	40	40–45	1	1.11	657	732	12.3	18900	28.77
	21–50	41	40–45	2	1.85	635	1175	11.89	26900	42.36
	51–100	46	40–47	3	3.06	1297	3969	24.29	108800	83.88
	101–450	47	40–55	5	5.89	780	4598	14.61	136600	175.13
	451–1000	46	40–59	6	10.25[a]	225	2307	4.21	75030	333.47
	1001–2867	48	40–56	Not determined[a]	20.20	29	586	0.54	21000	724.14
Total						3623	13367	67.84	387230	–

[a] The criteria for identification of an internal mechanism initiated AE are not satisfied.

likely to be responsible for generation and release of this type of AE waves.

Stage 3 of our AE monitoring is determined by a long time interval of an 11 h (Fig. 2a) with a very low AE activity (Table 4). The phenomenon observed during this stage can be associated with the Kaiser's effect [38] in cement-based materials observed during the loading–unloading cycles of the structures [14,37]. Thus within our cement specimen the stresses induced by further accumulation of corrosion products causing microcrack nucleation and development generated again AE activity after a long period of time, when the initial loading (suggested by the AE activity from the second stage) has been exceeded. This assumption is additionally verified by the results of the analysis applied for the AE hits from the last stage 4.

Table 6
AE characteristics for the signals detected from the reference cement sample

Time period	Hits duration (μs)	Amplitude peak (dB)	Amplitude range (dB)	Maximum no. of counts/hits	Calculated average counts/hits	N_{hits}	N_{counts}	% of total N_{hits}	Total E_{ABS} (aJ)	$E_{ABS,av}$ (aJ)
A (0–15.5 h)	0–1	43	40–49	1	1.67	203	338	3.74	271	1.33
	2–3	44	41–52	3	3.95	292	1153	5.38	1296	4.44
	4–16	45	41–54	5	6.03[a]	40	241	0.74	278	6.95
	17–400	46	41–55	3	12.34[a]	168	2074	3.1	3320	19.76
	401–615	50	43–55	12	123.6[a]	30	3708	0.55	5320	177.33
Total						733	7514	13.51	10485	–
B (15.5–25 h)	0–1	44	40–51	2	2.3	505	1162	9.31	1100	2.18
	2–3	46	41–53	5	3.87	398	1540	7.34	2180	5.48
	4–16	Not determined[a]	41–55	Not determined[a]	5.84	262	1531	4.83	3160	12.06
	17–400	Not determined[a]	41–55	Not determined[a]	9.93	1184	11759	21.83	23200	19.59
	401–618	51	41–55	7	20.75[a]	519	10773	9.57	20700	39.88
Total						2868	26765	52.88	50340	–
C (25–51.5 h)	0–1	43	40–51	2	2.09	419	876	7.73	686	1.64
	2–3	45	41–53	4	4.05	560	2266	10.33	2820	5.04
	4–16	Not determined[a]	41–55	1	[a]5.06	165	835	3.04	1660	10.06
	17–400	45	41–55	2	[a]11.08	617	6836	11.38	13100	21.23
	401–612	Not determined[a]	43–55	Not determined[a]	104.37	61	6367	1.13	13700	224.5
Total						1822	17180	33.61	31966	–

[a] The criteria for identification of an internal mechanism initiated AE are not satisfied.

Stage 4 constituted of a large number of short signals with duration between 0 and 50 μs and amplitude peak of 40 and 41 dB (Table 5). Moreover AE signals with duration between 51 and 450 μs and amplitude peak of 46 and 47 dB also were in high population during this stage. The later finding suggests appearing of several events such as microcrack nucleation and propagation in result of accumulation of a great amount of corrosion products, hydrogen bubbles formation and evolution and infiltration of water within the cement matrix [25,26].

3.2. AE data analysis for the reference cement sample

AE data collected from the reference sample have been processed following the same procedure as for the cement sample with encapsulated Al. However the time distribution of the AE signals along with the amount of detected absolute energy have been used to distinguish three stages in the AE activity denoted as A, B and C with duration respectively from 0 to 15.5, 15.5 to 25 and 25 to 51.5 h of our test (Fig. 3). For each of these stages only the signals with very short duration in the range 0–1 and 2–3 μs can be classified based on the criteria defined in [16] (Table 6). As reported by Chotard et al. [33,34] the complex chemical processes of cement hydration result in the initiation of AE with diversified characteristics. They related the low amplitude and short duration AE signals with the chemical reactions between cement and water, empting the capillary cement network. However the more energetic AE signals with longer duration and higher amplitude can be associated with the growth of the crystalline phases in cement along with fitting of hydrates and microcracking due to stress induced shrinkage [31–34]. The later processes generate AE which indicate further hardening of the cement structure.

It can be seen from Table 6 that the AE activity during the stage B is characterised with the largest number of detected AE hits. The important finding is that the average absolute energy calculated for these signals is significantly lower than for the AE waves detected during the stages A and C. Therefore we can suppose that the source of this AE activity is the progressive chemical reactions between the water and cement [33]. The significant role of these reactions responsible for initiation of AE during the stage B can be additionally distinguished by detection of AE signals with higher average absolute energy during the stage C believed to be related to microcracking of the cement structure in result of hydration process development [32,33].

4. Discussion

Our results confirm the potential of AE technique for detection of microcrack formation and development due to corrosion of Al encapsulated in cement matrix. The increase of AE activity during the stage 2 of our test is an indication for cracking of the structure caused by initiation and development of Al corrosion. The later was followed by hydrogen bubbles evolution and damage extension characterised with a great AE activity during the last stage of the conducted AE monitoring. It is worth noting that the number of AE signals detected during the stage 2 (1603) is about 2.3 times smaller than that detected during the last stage of the test (3623). However the total absolute energy for the stage 2 is about 2.5 times higher than that for the stage 4. This significant difference between the number of AE hits (N_{hits}) and the amount of detected absolute energy (E_{ABS}) versus time is evidenced from Fig. 6. Therefore the application of the procedure for identification of the failure mechanisms initiating AE [16] can significantly contribute for the understanding and even prediction of the mechanical behavior of cement matrix immobilising Al. Furthermore an important difference between the AE activities detected from both cement samples has been performed by the comparison of the range of variation of the peak of amplitude, duration, counts number and total absolute energy given in Table 7. Although the cumulated number of AE hits is of the same order for both samples, the cumulated absolute energy is about 16 times higher for the cement sample with encapsulated Al compared with the reference cement sample.

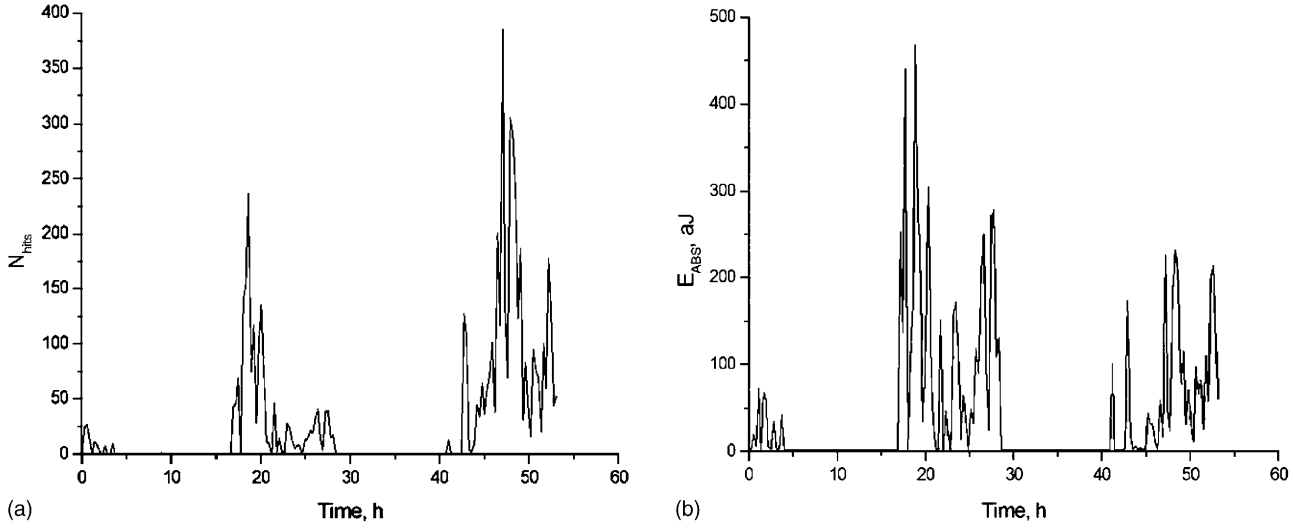

Fig. 6. Evolution of the total AE activity (a) and associated energy (b) vs. time for the cement sample with encapsulated Al.

Table 7
Characteristics of the detected AE hits form both cement samples

Amplitude (dB)	Duration (μs)	N_{counts}	Total N_{hits}	Total N_{counts}	Total E_{ABS} (aJ)	$E_{ABS,av}$ (aJ/hit)
Cement sample with encapsulated Al						
40–66	0–4650	0–50	5340	24485	1470109	275.3
Reference sample						
40–55	0–618	0–93	5423	51459	92791	17.11

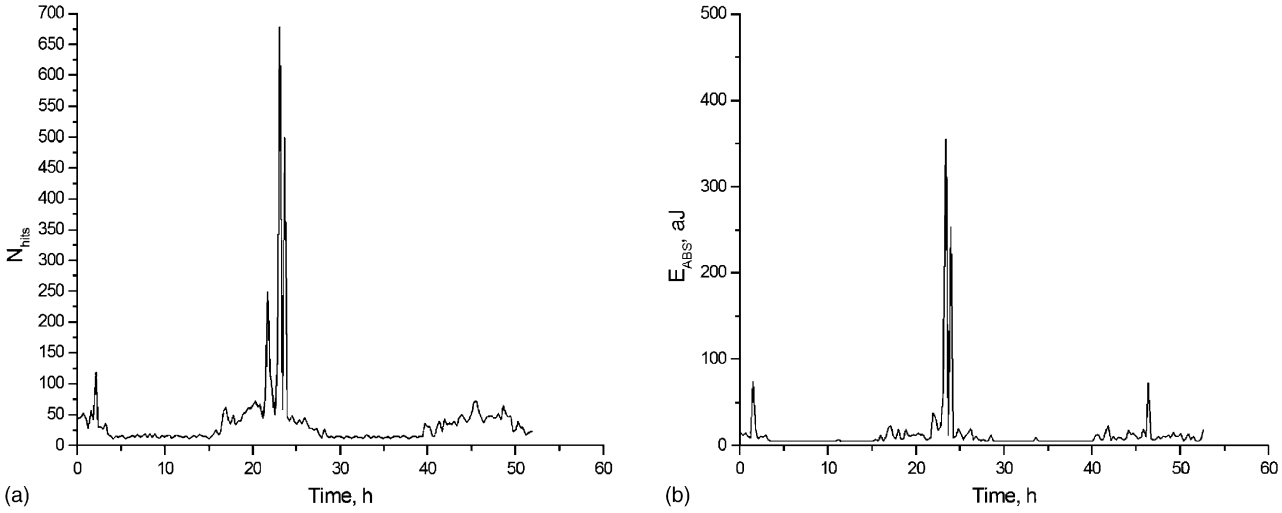

Fig. 7. Evolution of the total AE activity (a) and associated energy (b) vs. time for the reference cement sample.

Moreover from Fig. 7 it can be seen that the largest number of AE signals from the reference sample is associated with highest absolute energy detected. The later finding also is important in order to differentiate in term of AE the process of cement hydration and cracking type phenomena occurred in the cement structures under conducted AE monitoring.

5. Conclusions

Our study demonstrates that the AE technique can be used as a valuable tool for the continuous monitoring of microcrack formation and development within cementitious wasteforms encapsulating metallic wastes. The tendency of variation of the detected AE hits and amount of absolute energy is found to be similar with that reported from AE monitoring of cement-based structures during mechanical loading–unloading cycles. The experimental results indicate the presence of four different stages in the AE activity from the cement sample with encapsulated Al. The classification/differentiation procedure has been successfully used for ∼93% of the total number of AE signals from the cement sample with encapsulated Al. It demonstrated that processes associated with AE signals are infiltration of water through cement pores, accumulation of corrosion products followed by microcrack formation, onset of crack(s) and their extension, and hydrogen bubbles evolution. The comparative study of the AE data collected from the reference sample shows that the process of cement paste hardening is characterised with three time periods in the AE activity. Moreover detected AE signals are distinguished by acoustic characteristics such as amplitude, duration and counts number different from those detected from the cement sample with encapsulated Al.

Acknowledgements

We express our gratitude to Anthony Setiadi from the University of Sheffield for providing cement samples, Nexia Solutions and EPSRC Dorothy Hodgkin Postgraduate Award for funding. We also thank to N.B. Milestone, R.J. Hand and S. Morgan from the University of Sheffield for the helpful discussions.

References

[1] M.I. Ojovan, W.E. Lee, An Introduction to Nuclear Waste Immobilisation, Elsevier, Amsterdam, 2005.
[2] M. Atkins, F.P. Glasser, Application of Portland cement-based materials to radioactive waste immobilization, Waste Manage. 12 (1992) 105–131.
[3] J.H. Sharp, J. Hill, N.B. Milestone, E.W. Miller, Cementitious systems for encapsulation of intermediate level waste, in: Proceedings of the ICEM'03-4554: The 9th International Conference on Environmental Remediation and Radioactive Waste Management, Oxford, England, 2003.
[4] Q. Zhou, N.B. Milestone, M. Hayes, An alternative to Portland cement for waste encapsulation—the calcium sulfoaluminate cement system, J. Hazard. Mater. 136 (2006) 120–129.
[5] J. Li, J. Wang, Advances in cement solidification technology for waste radioactive ion exchange resins: a review, J. Hazard. Mater. B135 (2006) 443–448.
[6] A. Polettini, R. Pomi, P. Sirini, F. Testa, Properties of Portland cement-stabilised MSWI fly ashes, J. Hazard. Mater. 88 (1) (2001) 123–138.

[7] I. Plecas, R. Pavlovic, S. Pavlovic, Leaching behavior of ^{60}Co and ^{137}Cs from spent ion exchange resins in cement-bentonite clay matrix, J. Nucl. Mater. 327 (2004) 171–174.
[8] R. Streatfield, A review and update of the BNFL cement formulation development programme for the immobilisation of intermediate level wastes from Magnox power stations, in: Proceedings of the WM'01 Conference, Tucson, AZ, 2001.
[9] A. Setiadi, N.B. Milestone, M. Hayes, Corrosion of aluminium in composite cements, Extended Abstract, Cem. Concr. Sci. Conf., Warwick, 2004.
[10] A. Erdal Osmanlioglu, Immobilization of radioactive waste by cementation with purified kaolin clay, Waste Manage. 22 (2002) 481–483.
[11] M.A. Hamstad, A review: acoustic emission, a tool for composite materials studies, Exp. Mech. 26 (1986) 7–13.
[12] J. Roget, Acoustic emission: valuable applications and future trends, in: J.M. Farley, R.W. Nichols (Eds.), Proceedings of the Fourth European Conference on Non-destructive Testing, London, 1987.
[13] S.P. Shah, S. Choi, Nondestructive techniques for studying fracture processes in concrete, Int. J. Fracture 98 (3/4) (1999) 351–359.
[14] M.T. Tam, C.C. Weng, A study on acoustic emission characteristics of fly ash cement mortar under compression, Cem. Concr. Res. 24 (7) (1994) 1335–1346.
[15] E.N. Landis, L. Baillon, Experiments to relate acoustic emission energy to fracture energy of concrete, J. Eng. Mech. 128 (6) (2002) 698–702.
[16] K. Wu, B. Chen, W. Yao, Study of the AE characteristics of fracture process of mortar, concrete and steel–fiber–reinforced concrete beams, Cem. Concr. Res. 30 (2000) 1495–1500.
[17] M. Ohtsu, T. Okamoto, S. Yuyama, Moment tensor analysis of acoustic emission for cracking mechanisms in concrete, ACI Struct. J. 95 (2) (1998) 87–95.
[18] M. Ohtsu, Y. Kaminaga, M.C. Munwam, Experimental and numerical crack analysis of mixed-mode failure in concrete by acoustic emission and boundary element method, Constr. Build. Mater. 13 (1999) 57–64.
[19] M. Ohtsu, AE application to fracture mechanics, JCI Trans. 11 (1989) 673–678.
[20] E. Landis, Micro–macro fracture relationships and acoustic emission in concrete, Constr. Build. Mater. 13 (1999) 65–72.
[21] Z. Li, S.P. Shah, Microcracking in concrete under uniaxial tension, ACI Mater. J. 91 (4) (1994) 372–381.
[22] K. Wu, B. Chen, W. Yao, Study of the influence of aggregate size distribution on mechanical properties of concrete by acoustic emission technique, Cem. Concr. Res. 31 (2001) 919–923.
[23] B. Huet, V. L'Hostis, H. Idrissi, Use of acoustic emission to assess concrete reinforcement steel depassivation by chloride, EUROCORR 2003.
[24] M. Ing, S. Austin, R. Lyons, Cover zone properties influencing emission due to corrosion, Cem. Concr. Res. 35 (2005) 284–295.
[25] H. Idrissi, A. Limam, Study and characterization by acoustic emission and electrochemical measurements of concrete deterioration caused by reinforcement steel corrosion, NDT&E Int. 36 (2003) 563–569.
[26] B. Assouli, F. Simescu, G. Debicki, H. Idrissi, Detection and identification of concrete cracking during corrosion of reinforced concrete by acoustic emission coupled to the electrochemical techniques, NDT&E Int. 38 (2005) 682–689.
[27] H. Idrissi, J. Derenne, H. Mazille, Characterization and monitoring of pitting corrosion of aluminium alloys using the acoustic emission technique, EWGAE 2000.
[28] F. Bellenger, H. Mazille, H. Idrissi, Use of acoustic emission technique for the early detection of aluminium alloys exfoliation corrosion, NDT&E Int. 35 (2002) 385–392.
[29] H. Chang, E.H. Han, J.Q. Wang, W. Ke, Analysis of modal acoustic emission signals of LY12CZ aluminium alloy at anodic and cathodic polarization, NDT&E Int. 36 (2006) 8–12.
[30] M. Fregonese, H. Idrissi, H. Mazille, L. Renaud, Y. Cetre, Initiation and propagation steps in pitting corrosion of austenitic stainless steels: monitoring by acoustic emission, Corros. Sci. 43 (2001) 627–641.
[31] T. Shiotani, J. Bisschop, J.G.M. Van Mier, Temporal and spatial development of drying shrinkage cracking in cement-based materials, Eng. Fracture Mech. 70 (12) (2003) 1509–1525.
[32] V.R. Skal's'kyi, P.M. Koval', O.M. Serhienko, Yu.L. Lotots'kyi, Investigation of the solidification of concrete according to the signals of acoustic emission, Mater. Sci. 40 (5) (2004) 698–701.
[33] T.J. Chotard, A. Smith, D. Rotureau, D. Fargeot, C. Gault, Acoustic emission characterisation of calcium aluminate cement hydration at an early stage, J. Eur. Ceram. Soc. 35 (2003) 387–398.
[34] T.J. Chotard, D. Rotureau, A. Smith, Analysis of acoustic emission signature during aluminous cement setting to characterise the mechanical behaviour of the hard material, J. Eur. Ceram. Soc. 25 (2005) 3523–3531.
[35] A. Smith, T.J. Chotard, J.P. Bonnet, F. Louvet, C. Gault, Ultarasonic characterization of model mixtures of hydrated aluminious cement, J. Mater. Sci. 37 (2002) 3847–3853.
[36] V.Z. Belov, A.S. Aloy, Using acoustic emission in quality control of glass and ceramics for radioactive waste immobilization, Mater. Res. Soc. Symp. Proc. 807 (2004) 163–168.
[37] G.B. Muravin, V.V. Gur'ev, Kaiser effect and structural state of concrete, Soviet Journal of Nondestructive Testing (English translation of Defektoskopiya) 22 (10) (1986) 660–664.
[38] D.J. Holcomb, General theory of the Kaiser effect, Int. J. Rock Mech. Mining Sci. & Geomechanics Abstracts 30 (7) (1993) 929–935.